Interplay between spin polarization and color superconductivity in high density quark matter

Tsue, Yasuhiko; da Providência, João; Providência, Constança; Yamamura, Masatoshi; Bohr, Henrik

Published in:
Progress of Theoretical and Experimental Physics

Link to article, DOI:
10.1093/ptep/ptt076

Publication date:
2013

Document Version
Publisher's PDF, also known as Version of record

PTEP

Prog. Theor. Exp. Phys. **2013**, 103D01 (20 pages)
DOI: 10.1093/ptep/ptt076

Interplay between spin polarization and color superconductivity in high density quark matter

Yasuhiko Tsue[1,2,*], João da Providência[1,†], Constança Providência[1,†], Masatoshi Yamamura[3,†], and Henrik Bohr[4,†]

[1]*Center for Computational Physics, Departamento de Física, Universidade de Coimbra, 3004-516 Coimbra, Portugal*
[2]*Physics Division, Faculty of Science, Kochi University, Kochi 780-8520, Japan*
[3]*Department of Pure and Applied Physics, Faculty of Engineering Science, Kansai University, Suita 564-8680, Japan*
[4]*Department of Physics, B.307, Danish Technical University, DK-2800 Lyngby, Denmark*
[*]E-mail: tsue@kochi-u.ac.jp

Received November 27, 2012; Revised June 21, 2013; Accepted August 7, 2013; Published October 1, 2013

Here, it is suggested that a four-point interaction of the tensor type may lead to spin polarization in quark matter at high density. It is found that the two-flavor superconducting phase and the spin polarized phase correspond to distinct local minima of a certain generalized thermodynamical potential. It follows that a transition from one to the other phase occurs, passing through true minima with both a spin polarization and a color superconducting gap. It is shown that the quark spin polarized phase is realized at rather high density, while the two-flavor color superconducting phase is realized in a lower density region.

Subject Index D30

1. Introduction

Under extreme conditions, such as high temperature and/or high baryon density, it is interesting to study the behavior of quark and gluonic matter and/or hadronic matter governed by quantum chromodynamics (QCD) in the context of the physics of relativistic heavy ion collisions and of the interior of compact stars. In low temperature and high density regions [1] such as the interior of a neutron star, it has been widely investigated and pointed out that various phases may be realized, e.g., various meson condensed phases in hadronic matter [2], the two-flavor color superconducting (2SC) and color-flavor locked (CFL) phases [3–5], the quarkyonic phase [6], the quark ferromagnetic phase [7–9] in quark matter, and so forth. In particular, we may conjecture that the quark ferromagnetic phase exists at high density quark matter, since the existence of the magnetar was reported [10]. In preceding work [7–9], the pseudovector-type interaction between quarks was considered and it was pointed out that the quark spin polarization was realized. However, it was shown that the quark spin alignment disappears if the quark mass is zero, e.g., in the chiral symmetric phase [11]. Thus, it is interesting to investigate whether there is a possibility of spontaneous spin polarization under another interaction between quarks.

Recently, the present authors have indicated that the quark spin polarization may occur at high density quark matter even in the chiral symmetric phase due to the tensor-type four-point interaction

[†]These authors contributed equally to this work

between quarks, which leads to the quark spin polarization [12,13]. In these papers, it was shown that a second-order phase transition occurs from normal quark phase to quark spin polarized phase. However, in quark matter at high baryon density, it is believed that the two-flavor color superconducting phase appears. Thus, it is interesting to investigate the stability of the quark spin polarized phase against the 2SC phase.

In this paper, we investigate the color-symmetric superconducting phase [14] and the quark spin polarized phase and clarify which phase is stable by using the Nambu–Jona-Lasinio (NJL) model [15,16], including quark-pair interaction [17] and the tensor-type four-point interaction [12,13]. The quark-pair interaction is derived by a Fierz transformation from the original NJL model Lagrangian. As for the color superconducting phase, many possibilities, such as the gapless superconducting phase, which is still controversial for realistic situations, have been considered. However, in this paper, the simple 2SC phase derived by the NJL model is treated. We thus consider the quark-pairing gap Δ and the quark spin polarization F such that $\Delta \neq 0$ and/or $F \neq 0$ leads to the 2SC phase and/or quark spin polarized phase, respectively. In this paper, the system is treated by the mean field approximation and the BCS state is introduced [18].

This paper is organized as follows: In the next section, the basic Hamiltonian is introduced and expressions of the Hamiltonian under some basis sets are given. In Appendix A, one of the expressions of the Hamiltonian is given, in which good helicity states are used. In Sect. 3, the BCS state is defined, where a detailed derivation is given in Appendix B, and the thermodynamic potential is derived. In Sect. 4, numerical results and discussions are given, together with Appendix C, and the last section is devoted to a summary and concluding remarks.

2. NJL model with tensor interaction

2.1. Basic Hamiltonian

Let us start with the following Lagrangian density:

$$\begin{aligned}
\mathcal{L} &= \mathcal{L}_0 + \mathcal{L}_S + \mathcal{L}_T + \mathcal{L}_c, \\
\mathcal{L}_0 &= \bar{\psi} i\gamma^\mu \partial_\mu \psi, \\
\mathcal{L}_S &= G_S((\bar{\psi}\psi)^2 + (\bar{\psi} i\gamma_5 \vec{\tau}\psi)^2), \\
\mathcal{L}_T &= -\frac{G}{4}\left((\bar{\psi}\gamma^\mu\gamma^\nu\vec{\tau}\psi)(\bar{\psi}\gamma_\mu\gamma_\nu\vec{\tau}\psi) + (\bar{\psi} i\gamma_5\gamma^\mu\gamma^\nu\psi)(\bar{\psi} i\gamma_5\gamma_\mu\gamma_\nu\psi)\right), \\
\mathcal{L}_c &= \frac{G_c}{2}\sum_{A=2,5,7}\left((\bar{\psi} i\gamma_5\tau_2\lambda_A\psi^C)(\bar{\psi}^C i\gamma_5\tau_2\lambda_A\psi) + (\bar{\psi}\tau_2\lambda_A\psi^C)(\bar{\psi}^C\tau_2\lambda_A\psi)\right).
\end{aligned} \tag{1}$$

Here, $\psi^C = C\bar{\psi}^T$ with $C = i\gamma^2\gamma^0$ being the charge conjugation operator. Also, τ_2 is the second component of the Pauli matrices representing the isospin $su(2)$-generator and λ_A are the antisymmetric Gell–Mann matrices representing the color $su(3)_c$-generator. As is well known, the Lagrangian density $\mathcal{L}_0 + \mathcal{L}_S$ corresponds to the original NJL model. We add $\mathcal{L}_c$, which can be derived by the Fierz transformation from $\mathcal{L}_S$, and which represents the quark-pair interaction. Also, we introduce $\mathcal{L}_T$, which represents the tensor-type interaction between quarks.

In this paper, we concentrate on quark matter at high baryon density where the chiral symmetry is restored in the density region considered here. Thus, the chiral condensate, $\langle\bar{\psi}\psi\rangle$, is assumed to be

equal to zero in this high density region. Under the mean field approximation, the above Lagrangian density is recast into

$$\begin{aligned}
\mathcal{L}^{\rm MF} &= \mathcal{L}_0 + \mathcal{L}_T^{\rm MF} + \mathcal{L}_c^{\rm MF},\\
\mathcal{L}_T^{\rm MF} &= -F(\bar\psi\Sigma_3\tau_3\psi) - \frac{F^2}{2G},\\
F &= -G\langle\bar\psi\Sigma_3\tau_3\psi\rangle, \quad \Sigma_3 = -i\gamma^1\gamma^2 = \begin{pmatrix}\sigma_3 & 0\\ 0 & \sigma_3\end{pmatrix},\\
\mathcal{L}_c^{\rm MF} &= -\frac{1}{2}\sum_{A=2,5,7}(\Delta\bar\psi^C i\gamma_5\tau_2\lambda_A + \text{h.c.}) - \frac{3\Delta^2}{2G_c},\\
\Delta_A &= \Delta_A^* = -G_c\langle\bar\psi i\gamma_5\tau_2\lambda_A\psi\rangle, \quad \Delta = \Delta_2 = \Delta_5 = \Delta_7,
\end{aligned} \tag{2}$$

where $h.c.$ represents the Hermitian conjugate term of the preceding one. Here, we have used a Dirac representation for the Dirac gamma matrices and σ_3 represents the third component of the 2×2 Pauli spin matrices. The symbol $\langle\cdots\rangle$ represents the expectation value with respect to a vacuum state. The expectation value F corresponds to the order parameter of the spin alignment that leads to quark ferromagnetization. The expectation value Δ corresponds to the quark-pair condensate, which means the existence of the color superconducting phase if $\Delta \neq 0$. Here, in order to ensure color symmetry, we assume that all quark-pair condensates have the same expectation values, $\Delta_2 = \Delta_5 = \Delta_7$.

The mean field Hamiltonian density with quark chemical potential μ is easily obtained as

$$\begin{aligned}
\mathcal{H}_{\rm MF} - \mu\mathcal{N} &= \mathcal{K}_0 + \mathcal{H}_T^{\rm MF} + \mathcal{H}_c^{\rm MF},\\
\mathcal{K}_0 &= \bar\psi(-\boldsymbol{\gamma}\cdot\nabla - \mu\gamma_0)\psi,\\
\mathcal{H}_T^{\rm MF} &= -\mathcal{L}_T^{\rm MF}, \quad \mathcal{H}_c^{\rm MF} = -\mathcal{L}_c^{\rm MF}
\end{aligned} \tag{3}$$

with $\mathcal{N} = \psi^\dagger\psi$. In the Dirac representation for the Dirac gamma matrices, the Hamiltonian matrix of the spin polarization part, $H_{\rm MF}^{\rm SP} = \int d^3\boldsymbol{x}\,(\mathcal{K}_0 + \mathcal{H}_T^{\rm MF})$, is written as

$$\begin{aligned}
h_{\rm MF}^{\rm SP} &= \boldsymbol{p}\cdot\boldsymbol{\alpha} + F\tau_3\beta\Sigma_3\\
&= \begin{pmatrix} F\tau_3 & 0 & p_3 & p_1 - ip_2\\ 0 & -F\tau_3 & p_1 + ip_2 & p_3\\ p_3 & p_1 - ip_2 & -F\tau_3 & 0\\ p_1 + ip_2 & -p_3 & 0 & F\tau_3\end{pmatrix},
\end{aligned} \tag{4}$$

where $\alpha^i = \gamma^0\gamma^i$ and $\beta = \gamma^0$. For good helicity states, this Hamiltonian matrix is diagonalized with $F = 0$. For simplicity, we rotate around the p_3 axis and we set $p_2 = 0$ without loss of generality. In this case, we derive $\kappa = U^{-1}h_{\rm MF}^{\rm SP}U$ as follows:

$$U = \frac{1}{2\sqrt{p}}\begin{pmatrix} \sqrt{p+p_3} & \sqrt{p-p_3} & -\sqrt{p+p_3} & -\sqrt{p-p_3}\\ \frac{p_1}{|p_1|}\sqrt{p-p_3} & -\frac{p_1}{|p_1|}\sqrt{p+p_3} & -\frac{p_1}{|p_1|}\sqrt{p-p_3} & \frac{p_1}{|p_1|}\sqrt{p+p_3}\\ \sqrt{p+p_3} & -\sqrt{p-p_3} & \sqrt{p+p_3} & -\sqrt{p-p_3}\\ \frac{p_1}{|p_1|}\sqrt{p-p_3} & \frac{p_1}{|p_1|}\sqrt{p+p_3} & \frac{p_1}{|p_1|}\sqrt{p-p_3} & \frac{p_1}{|p_1|}\sqrt{p+p_3}\end{pmatrix},$$

$$\kappa = U^{-1} h_{\rm MF}^{\rm SP} U$$
$$= \begin{pmatrix} p & 0 & 0 & 0 \\ 0 & p & 0 & 0 \\ 0 & 0 & -p & 0 \\ 0 & 0 & 0 & -p \end{pmatrix} + \frac{F\tau_3}{p} \begin{pmatrix} 0 & |p_1| & -p_3 & 0 \\ |p_1| & 0 & 0 & p_3 \\ -p_3 & 0 & 0 & |p_1| \\ 0 & p_3 & |p_1| & 0 \end{pmatrix}. \tag{5}$$

Finally, in the original basis rotated around the p_3-axis, $|p_1|$ is replaced with $\sqrt{p_1^2 + p_2^2}$. As for the Hamiltonian matrix of the color superconducting part, $H_c^{\rm MF} = \int d^3\boldsymbol{x} \mathcal{H}_c^{\rm MF}$, the result has already been obtained in Ref. [17], based on Ref. [14]. As a result, on the basis of good helicity states, the relevant combination of the mean field Hamiltonian $H_{\rm MF} = \int d^3\boldsymbol{x} \mathcal{H}_{\rm MF}$ and the quark number $N = \int d^3\boldsymbol{x} \mathcal{N}$ is given by

$$\begin{aligned} H_{\rm MF} - \mu N = & \sum_{\boldsymbol{p}\eta\tau\alpha} \left[(p-\mu) c^\dagger_{\boldsymbol{p}\eta\tau\alpha} c_{\boldsymbol{p}\eta\tau\alpha} - (p+\mu) \tilde{c}^\dagger_{\boldsymbol{p}\eta\tau\alpha} \tilde{c}_{\boldsymbol{p}\eta\tau\alpha} \right] \\ & + F \sum_{\boldsymbol{p}\eta\tau\alpha} \phi_\tau \left[\frac{\sqrt{p_1^2 + p_2^2}}{p} \left(c^\dagger_{\boldsymbol{p}\eta\tau\alpha} c_{\boldsymbol{p}-\eta\tau\alpha} + \tilde{c}^\dagger_{\boldsymbol{p}\eta\tau\alpha} \tilde{c}_{\boldsymbol{p}-\eta\tau\alpha} \right) \right. \\ & \qquad \left. - \eta \frac{p_3}{p} \left(c^\dagger_{\boldsymbol{p}\eta\tau\alpha} \tilde{c}_{\boldsymbol{p}\eta\tau\alpha} + \tilde{c}^\dagger_{\boldsymbol{p}\eta\tau\alpha} c_{\boldsymbol{p}\eta\tau\alpha} \right) \right] \\ & + \frac{\Delta}{2} \sum_{\boldsymbol{p}\eta\alpha\alpha'\alpha''\tau\tau'} (c^\dagger_{\boldsymbol{p}\eta\tau\alpha} c^\dagger_{-\boldsymbol{p}\eta\tau'\alpha'} + \tilde{c}^\dagger_{\boldsymbol{p}\eta\tau\alpha} \tilde{c}^\dagger_{-\boldsymbol{p}\eta\tau'\alpha'} \\ & \qquad + c_{-\boldsymbol{p}\eta\tau'\alpha'} c_{\boldsymbol{p}\eta\tau\alpha} + \tilde{c}_{-\boldsymbol{p}\eta\tau'\alpha'} \tilde{c}_{\boldsymbol{p}\eta\tau\alpha}) \phi_\tau \epsilon_{\alpha\alpha'\alpha''} \epsilon_{\tau\tau'} \\ & + V \cdot \frac{F^2}{2G} + V \cdot \frac{3\Delta^2}{2G_c}, \end{aligned} \tag{6}$$

where V represents the volume in the box normalization.[1] Here, $c^\dagger_{\boldsymbol{p}\eta\tau\alpha}$ and $\tilde{c}^\dagger_{\boldsymbol{p}\eta\tau\alpha}$ represent the quark and antiquark creation operators with momentum $\boldsymbol{p}$, helicity $\eta = \pm$, isospin index $\tau = \pm$, and color α. Further, $\phi_\tau = 1$ for $\tau = 1$ (up quark) and $\phi_\tau = -1$ for $\tau = -1$ (down quark). Also, $\epsilon_{\tau\tau'}$ and $\epsilon_{\alpha\alpha'\alpha''}$ represent the complete antisymmetric tensor for the isospin and color indices. We define $p = \sqrt{p_1^2 + p_2^2 + p_3^2}$, i.e., the magnitude of momentum.

For later convenience, we rewrite the above Hamiltonian as

$$H_{\rm MF} - \mu N = H_{\rm MF}^{\rm SP} - \mu N + V_{cs} + V \cdot \frac{F^2}{2G} + V \cdot \frac{3\Delta^2}{2G_c} \tag{7}$$

with

$$H_{\rm MF}^{\rm SP} - \mu N = \sum_{\boldsymbol{p}\tau\tau'\alpha\alpha'\alpha''} \begin{pmatrix} c^\dagger_{\boldsymbol{p}+\tau\alpha} \\ c^\dagger_{\boldsymbol{p}-\tau\alpha} \\ \tilde{c}^\dagger_{\boldsymbol{p}+\tau\alpha} \\ \tilde{c}^\dagger_{\boldsymbol{p}-\tau\alpha} \end{pmatrix}^T (\kappa - \mu \cdot 1) \delta_{\tau\tau'} \delta_{\alpha\alpha'} \begin{pmatrix} c_{\boldsymbol{p}+\tau'\alpha'} \\ c_{\boldsymbol{p}-\tau'\alpha'} \\ \tilde{c}_{\boldsymbol{p}+\tau'\alpha'} \\ \tilde{c}_{\boldsymbol{p}-\tau'\alpha'} \end{pmatrix},$$

[1] We hope that no confusion will occur, although notations V_{cs} and $V(\boldsymbol{p})$ appear later, which represent the quark-pair interaction in (7) and a matrix in (A1) diagonalizing a certain part of the Hamiltonian matrix, respectively.

$$\kappa = \begin{pmatrix} p & 0 & 0 & 0 \\ 0 & p & 0 & 0 \\ 0 & 0 & -p & 0 \\ 0 & 0 & 0 & -p \end{pmatrix} + \frac{F\tau_3}{p} \begin{pmatrix} 0 & \sqrt{p_1^2+p_2^2} & -p_3 & 0 \\ \sqrt{p_1^2+p_2^2} & 0 & 0 & p_3 \\ -p_3 & 0 & 0 & \sqrt{p_1^2+p_2^2} \\ 0 & p_3 & \sqrt{p_1^2+p_2^2} & 0 \end{pmatrix},$$

$$V_{cs} = \frac{\Delta}{2} \sum_{\boldsymbol{p}\eta\alpha\alpha'\alpha''\tau\tau'} (c^\dagger_{\boldsymbol{p}\eta\tau\alpha} c^\dagger_{-\boldsymbol{p}\eta\tau'\alpha'} + \tilde{c}^\dagger_{\boldsymbol{p}\eta\tau\alpha} \tilde{c}^\dagger_{-\boldsymbol{p}\eta\tau'\alpha'} + c_{-\boldsymbol{p}\eta\tau'\alpha'} c_{\boldsymbol{p}\eta\tau\alpha} + \tilde{c}_{-\boldsymbol{p}\eta\tau'\alpha'} \tilde{c}_{\boldsymbol{p}\eta\tau\alpha}) \times \phi_\tau \epsilon_{\alpha\alpha'\alpha''} \epsilon_{\tau\tau'}. \tag{8}$$

As for V_{cs}, we can easily sum up with respect to τ and τ', which leads to

$$V_{cs} = \Delta \sum_{\boldsymbol{p}\eta\alpha\alpha'\alpha''} \epsilon_{\alpha\alpha'\alpha''} (c^\dagger_{\boldsymbol{p}\eta+\alpha} c^\dagger_{-\boldsymbol{p}\eta-\alpha'} + \tilde{c}^\dagger_{\boldsymbol{p}\eta+\alpha} \tilde{c}^\dagger_{-\boldsymbol{p}\eta-\alpha'} + c_{-\boldsymbol{p}\eta-\alpha'} c_{\boldsymbol{p}\eta+\alpha} + \tilde{c}_{-\boldsymbol{p}\eta-\alpha'} \tilde{c}_{\boldsymbol{p}\eta+\alpha}). \tag{9}$$

2.2. *Expressions of the Hamiltonian under other basis sets*

If the quark-pair condensate Δ is equal to zero, the operator given by Eq. (7) becomes $H^{\rm SP}_{\rm MF} - \mu N + VF^2/(2G)$. Since the quark number N is already diagonal, let us diagonalize the Hamiltonian matrix κ. First, we set up $\tau_3 = 1$ because the contribution of $\tau_3 = -1$ is the same as the contribution of $\tau_3 = 1$, as was seen in (9), which results in a factor 2. Then, the Hamiltonian matrix κ can be simply expressed as

$$\kappa = \begin{pmatrix} q & e & -g & 0 \\ e & q & 0 & g \\ -g & 0 & -q & e \\ 0 & g & e & -q \end{pmatrix}, \tag{10}$$

where $q = p$, $e = F\sqrt{p_1^2+p_2^2}/p$ and $g = Fp_3/p$. The eigenvalues of κ are easily obtained as

$$\pm\varepsilon^{(\pm)}_{\boldsymbol{p}} = \pm\sqrt{g^2+(e\pm q)^2} = \pm\sqrt{p_3^2 + \left(F \pm \sqrt{p_1^2+p_2^2}\right)^2}. \tag{11}$$

By introducing new fermion operators $(a_{\boldsymbol{p}\eta\tau\alpha}, a^\dagger_{\boldsymbol{p}\eta\tau\alpha}, \tilde{a}_{\boldsymbol{p}\eta\tau\alpha}, \tilde{a}^\dagger_{\boldsymbol{p}\eta\tau\alpha})$ by

$$\begin{pmatrix} a_{\boldsymbol{p}+\tau\alpha} \\ a_{\boldsymbol{p}-\tau\alpha} \\ \tilde{a}_{\boldsymbol{p}+\tau\alpha} \\ \tilde{a}_{\boldsymbol{p}-\tau\alpha} \end{pmatrix} = W^\dagger V^\dagger(\boldsymbol{p}) \begin{pmatrix} c_{\boldsymbol{p}+\tau\alpha} \\ c_{\boldsymbol{p}-\tau\alpha} \\ \tilde{c}_{\boldsymbol{p}+\tau\alpha} \\ \tilde{c}_{\boldsymbol{p}-\tau\alpha} \end{pmatrix}, \tag{12}$$

where the operators $V(\boldsymbol{p})$ and W are given in Appendix A, the mean field Hamiltonian in which both quark spin polarization and the quark-pair condensate are simultaneously considered can be expressed as

$$\begin{aligned} H_{\rm MF} - \mu N = & \sum_{\boldsymbol{p}\eta\tau\alpha} \left[(\varepsilon^{(\eta)}_{\boldsymbol{p}} - \mu) a^\dagger_{\boldsymbol{p}\eta\tau\alpha} a_{\boldsymbol{p}\eta\tau\alpha} - (\varepsilon^{(\eta)}_{\boldsymbol{p}} + \mu) \tilde{a}^\dagger_{\boldsymbol{p}\eta\tau\alpha} \tilde{a}_{\boldsymbol{p}\eta\tau\alpha} \right] \\ & + \frac{\Delta}{2} \sum_{\boldsymbol{p}\eta\tau\tau'\alpha\alpha'\alpha''} \left[a^\dagger_{\boldsymbol{p}\eta\tau\alpha'} a^\dagger_{-\boldsymbol{p}\eta\tau'\alpha''} - \tilde{a}^\dagger_{\boldsymbol{p}\eta\tau\alpha'} \tilde{a}^\dagger_{-\boldsymbol{p}\eta\tau\alpha''} + h.c. \right] \epsilon_{\alpha\alpha'\alpha''} \epsilon_{\tau\tau'} \phi_\tau \\ & + V \cdot \frac{F^2}{2G} + V \cdot \frac{3\Delta^2}{2G_c}. \end{aligned} \tag{13}$$

Here, the summation with respect to isospin indices τ and τ' is explicitly rewritten. The above mean field Hamiltonian is the starting point for discussing the quark spin polarized phase and color superconducting phase.

3. BCS state and thermodynamic potential

We introduce the BCS state following Ref. [18]:

$$
\begin{aligned}
|\Psi\rangle = e^S|\Psi_0\rangle, \quad |\Psi_0\rangle &= \prod_{\boldsymbol{p}\eta\tau\alpha(\varepsilon_{\boldsymbol{p}}^{(\eta)}<\mu)} a^\dagger_{\boldsymbol{p}\eta\tau\alpha}|0\rangle, \\
S &= \sum_{\boldsymbol{p}\eta(\varepsilon_{\boldsymbol{p}}^{(\eta)}>\mu)} \frac{K_{\boldsymbol{p}\eta}}{2} \sum_{\alpha\alpha'\alpha''\tau\tau'} a^\dagger_{\boldsymbol{p}\eta\tau\alpha} a^\dagger_{-\boldsymbol{p}\eta\tau'\alpha'} \epsilon_{\alpha\alpha'\alpha''}\epsilon_{\tau\tau'}\phi_\tau \\
&\quad + \sum_{\boldsymbol{p}\eta(\varepsilon_{\boldsymbol{p}}^{(\eta)}\le\mu)} \frac{\widetilde{K}_{\boldsymbol{p}\eta}}{2} \sum_{\alpha\alpha'\alpha''\tau\tau'} a_{\boldsymbol{p}\eta\tau\alpha} a_{-\boldsymbol{p}\eta\tau'\alpha'} \epsilon_{\alpha\alpha'\alpha''}\epsilon_{\tau\tau'}\phi_\tau,
\end{aligned}
\tag{14}
$$

where $|0\rangle$ is the vacuum state with respect to $a_{\boldsymbol{p}\eta\tau\alpha}$, and $K_{\boldsymbol{p}\eta} = K_{-\boldsymbol{p}\eta}$ and $\widetilde{K}_{\boldsymbol{p}\eta} = \widetilde{K}_{-\boldsymbol{p}\eta}$ are satisfied. Here, the contribution of quark-pairing with negative energy is not considered in quark matter. Then, the state $|\Psi\rangle$ is a vacuum state with respect to new operators $d_{\boldsymbol{p}\eta\tau\alpha}$:

$$
d_{\boldsymbol{p}\eta\tau\alpha} = \begin{cases} a_{\boldsymbol{p}\eta\tau\alpha} - K_{\boldsymbol{p}\eta}(a^\dagger_{-\boldsymbol{p}\eta\tau'\beta} - a^\dagger_{-\boldsymbol{p}\eta\tau'\gamma}) & \text{for} \quad \varepsilon_{\boldsymbol{p}}^{(\eta)} > \mu \\ a^\dagger_{\boldsymbol{p}\eta\tau\alpha} + \widetilde{K}_{\boldsymbol{p}\eta}(a_{-\boldsymbol{p}\eta\tau'\beta} - a_{-\boldsymbol{p}\eta\tau'\gamma}) & \text{for} \quad \varepsilon_{\boldsymbol{p}}^{(\eta)} \le \mu \end{cases},
\tag{15}
$$

where (α, β, γ) is a cyclic permutation for color indices and $\tau' = -\tau$. For the above operators, the state $|\Psi\rangle$ satisfies the following relation:

$$
d_{\boldsymbol{p}\eta\tau\alpha}|\Psi\rangle = 0.
\tag{16}
$$

The state $|\Psi\rangle$ is identical with the BCS state.

In order to calculate the expectation value of the mean field Hamiltonian (13), it is necessary to obtain the expectation values of $a^\dagger_{\boldsymbol{p}\eta\tau\alpha}a_{\boldsymbol{p}\eta\tau\alpha}$, $a^\dagger_{\boldsymbol{p}\eta\tau\alpha}a^\dagger_{-\boldsymbol{p}\eta\tau'\alpha'}$, and so on with respect to the BCS state $|\Psi\rangle$. The detailed calculations are given in Appendix B. Thus, by summing up with respect to color and isospin indices, we obtain the expectation value of the mean field Hamiltonian for the BCS state as

$$
\begin{aligned}
\langle\Psi|H_{\mathrm{MF}} - \mu N|\Psi\rangle &= 3 \sum_{\boldsymbol{p}\eta\tau(\varepsilon_{\boldsymbol{p}}^{(\eta)}>\mu)} \left[(\varepsilon_{\boldsymbol{p}}^{(\eta)} - \mu)\frac{2K^2_{\boldsymbol{p}\eta}}{1+3K^2_{\boldsymbol{p}\eta}} + 2\Delta\frac{K_{\boldsymbol{p}\eta}}{1+3K^2_{\boldsymbol{p}\eta}} \right] \\
&\quad + 3 \sum_{\boldsymbol{p}\eta\tau(\varepsilon_{\boldsymbol{p}}^{(\eta)}\le\mu)} \left[(\varepsilon_{\boldsymbol{p}}^{(\eta)} - \mu)\left(1 - \frac{2\widetilde{K}^2_{\boldsymbol{p}\eta}}{1+3\widetilde{K}^2_{\boldsymbol{p}\eta}}\right) + 2\Delta\frac{\widetilde{K}_{\boldsymbol{p}\eta}}{1+3\widetilde{K}^2_{\boldsymbol{p}\eta}} \right] \\
&\quad + V\cdot\frac{F^2}{2G} + V\cdot\frac{3\Delta^2}{2G_c}.
\end{aligned}
\tag{17}
$$

In order to determine the BCS state, namely, to determine the variational variables $K_{\boldsymbol{p}\eta}$ and $\widetilde{K}_{\boldsymbol{p}\eta}$, we introduce new variational variables $\theta_{p\eta}$ and $\tilde{\theta}_{p\eta}$ instead of $K_{\boldsymbol{p}\eta}$ and $\widetilde{K}_{\boldsymbol{p}\eta}$:

$$\sin\theta_{p\eta} = \frac{\sqrt{3}K_{\boldsymbol{p}\eta}}{\sqrt{1+3K_{\boldsymbol{p}\eta}^2}}, \quad \cos\theta_{p\eta} = \frac{1}{\sqrt{1+3K_{\boldsymbol{p}\eta}^2}},$$
$$\sin\tilde{\theta}_{p\eta} = \frac{\sqrt{3}\widetilde{K}_{\boldsymbol{p}\eta}}{\sqrt{1+3\widetilde{K}_{\boldsymbol{p}\eta}^2}}, \quad \cos\tilde{\theta}_{p\eta} = \frac{1}{\sqrt{1+3\widetilde{K}_{\boldsymbol{p}\eta}^2}}. \tag{18}$$

Thus, the Hamiltonian and color superconducting gap Δ can be expressed in terms of $\theta_{p\eta}$ and $\tilde{\theta}_{p\eta}$ as

$$\begin{aligned}\langle\Psi|H_{\rm MF}-\mu N|\Psi\rangle &= 2\sum_{\boldsymbol{p}\eta(\varepsilon_{\boldsymbol{p}}^{(\eta)}>\mu)}\left[2(\varepsilon_{\boldsymbol{p}}^{(\eta)}-\mu)\sin^2\theta_{p\eta}+2\sqrt{3}\Delta\sin\theta_{p\eta}\cos\theta_{p\eta}\right]\\ &\quad+2\sum_{\boldsymbol{p}\eta(\varepsilon_{\boldsymbol{p}}^{(\eta)}\le\mu)}\left[(\varepsilon_{\boldsymbol{p}}^{(\eta)}-\mu)(3-2\sin^2\tilde{\theta}_{p\eta})+2\sqrt{3}\Delta\sin\tilde{\theta}_{p\eta}\cos\tilde{\theta}_{p\eta}\right]\\ &\quad+V\cdot\frac{F^2}{2G}+V\cdot\frac{3\Delta^2}{2G_c},\end{aligned} \tag{19}$$

$$\begin{aligned}\Delta=\Delta_2=\Delta_5=\Delta_7 &= -G_c\cdot\frac{1}{V}\sum_{\boldsymbol{p}\eta\beta\gamma\tau}\langle\Psi|a^\dagger_{\boldsymbol{p}\eta\tau\beta}a^\dagger_{-\boldsymbol{p}\eta-\tau\gamma}|\Psi\rangle\\ &= -2G_c\left(\frac{1}{V}\sum_{\boldsymbol{p}\eta\tau(\varepsilon_{\boldsymbol{p}}^{(\eta)}>\mu)}\frac{K_{\boldsymbol{p}\eta}}{1+3K_{\boldsymbol{p}\eta}^2}+\frac{1}{V}\sum_{\boldsymbol{p}\eta\tau(\varepsilon_{\boldsymbol{p}}^{(\eta)}\le\mu)}\frac{\widetilde{K}_{\boldsymbol{p}\eta}}{1+3\widetilde{K}_{\boldsymbol{p}\eta}^2}\right)\\ &= -\frac{4G_c}{\sqrt{3}}\left(\frac{1}{V}\sum_{\boldsymbol{p}\eta(\varepsilon_{\boldsymbol{p}}^{(\eta)}>\mu)}\sin\theta_{p\eta}\cos\theta_{p\eta}+\frac{1}{V}\sum_{\boldsymbol{p}\eta(\varepsilon_{\boldsymbol{p}}^{(\eta)}\le\mu)}\sin\tilde{\theta}_{p\eta}\cos\tilde{\theta}_{p\eta}\right).\end{aligned} \tag{20}$$

Here, in the first line in (19) and the third line in (20), the isospin indices are summed up and an extra factor 2 appears with respect to the corresponding expression in Ref. [14]. Also, in the second line in (20), the color indices β and γ are summed up and an extra factor 2 also appears.

Next, we impose the minimization condition for $\langle\Psi|H_{\rm MF}-\mu N|\Psi\rangle$ with respect to Δ, $\theta_{p\eta}$, and $\tilde{\theta}_{p\eta}$. First, we impose the minimization condition with respect to Δ:

$$\frac{\partial}{\partial\Delta}\langle\Psi|H_{\rm MF}-\mu N|\Psi\rangle = 0. \tag{21}$$

This minimization condition leads to the gap equation in (20) exactly. Secondly, we minimize $\langle\Psi|H_{\rm MF}-\mu N|\Psi\rangle$ with respect to $\theta_{p\eta}$ and $\tilde{\theta}_{p\eta}$:

$$\frac{\partial}{\partial\theta_{p\eta}}\langle\Psi|H_{\rm MF}-\mu N|\Psi\rangle = 0, \quad \frac{\partial}{\partial\tilde{\theta}_{p\eta}}\langle\Psi|H_{\rm MF}-\mu N|\Psi\rangle = 0, \tag{22}$$

which lead to the following equations:

$$\begin{aligned}(\varepsilon_{\boldsymbol{p}}^{(\eta)}-\mu)\sin 2\theta_{p\eta}+\sqrt{3}\Delta\cos 2\theta_{p\eta}=0,\\ -(\varepsilon_{\boldsymbol{p}}^{(\eta)}-\mu)\sin 2\tilde{\theta}_{p\eta}+\sqrt{3}\Delta\cos 2\tilde{\theta}_{p\eta}=0.\end{aligned} \tag{23}$$

Thus, we obtain $\tan 2\theta_{p\eta}=-\sqrt{3}\Delta/(\varepsilon_{\boldsymbol{p}}^{(\eta)}-\mu)$ and $\tan 2\tilde{\theta}_{p\eta}=\sqrt{3}\Delta/(\varepsilon_{\boldsymbol{p}}^{(\eta)}-\mu)$, which gives

$$\begin{aligned}\sin\theta_{p\eta}^2&=\frac{1}{2}\left[1-\frac{\varepsilon_{\boldsymbol{p}}^{(\eta)}-\mu}{\sqrt{(\varepsilon_{\boldsymbol{p}}^{(\eta)}-\mu)^2+3\Delta^2}}\right],\\ \sin\tilde{\theta}_{p\eta}^2&=\frac{1}{2}\left[1+\frac{\varepsilon_{\boldsymbol{p}}^{(\eta)}-\mu}{\sqrt{(\varepsilon_{\boldsymbol{p}}^{(\eta)}-\mu)^2+3\Delta^2}}\right].\end{aligned} \tag{24}$$

Since the variational parameters $\theta_{p\eta}$ and $\tilde{\theta}_{p\eta}$ are determined completely, namely, $K_{\boldsymbol{p}\eta}$ and $\widetilde{K}_{\boldsymbol{p}\eta}$ are determined, the BCS state is obtained.

Thus, we can derive the thermodynamic potential $\Phi(\Delta, F, \mu)$ at zero temperature from (19) with (24) as

$$\begin{aligned}\Phi(\Delta,F,\mu)&=\frac{1}{V}\langle\Phi|H_{\mathrm{MF}}-\mu N|\Phi\rangle\\ &=2\cdot\frac{1}{V}\sum_{\boldsymbol{p}\eta(\varepsilon_{\boldsymbol{p}}^{(\eta)}\le\mu)}\left[2(\varepsilon_{\boldsymbol{p}}^{(\eta)}-\mu)-\sqrt{(\varepsilon_{\boldsymbol{p}}^{(\eta)}-\mu)^2+3\Delta^2}\right]\\ &\quad+2\cdot\frac{1}{V}\sum_{\boldsymbol{p}\eta(\varepsilon_{\boldsymbol{p}}^{(\eta)}>\mu)}^{\Lambda}\left[(\varepsilon_{\boldsymbol{p}}^{(\eta)}-\mu)-\sqrt{(\varepsilon_{\boldsymbol{p}}^{(\eta)}-\mu)^2+3\Delta^2}\right]\\ &\quad+\frac{F^2}{2G}+\frac{3\Delta^2}{2G_c},\end{aligned} \tag{25}$$

where $\varepsilon_{\boldsymbol{p}}^{(\pm)}=\sqrt{p_3^2+\left(F\pm\sqrt{p_1^2+p_2^2}\right)^2}$. Here, we explicitly introduce and write a three-momentum cutoff parameter Λ. The above derivation is nothing but that of the usual method in the BCS theory. Therefore, it is possible to derive the same result using the equations of motion by eliminating so-called dangerous terms in the algebraic method [18]. It may be interesting to observe that Eq. (25) means, physically, that only two "effective colors" participate in the pairing process, the third "color" remaining inert. The contribution of the active "colors" to the energy is $\left(2(\varepsilon_{\boldsymbol{p}}^{(\eta)}-\mu)-2\sqrt{(\varepsilon_{\boldsymbol{p}}^{(\eta)}-\mu)^2+3\Delta^2}\right)/2$, both for $\varepsilon_{\boldsymbol{p}}^{(\eta)}<\mu$ and for $\varepsilon_{\boldsymbol{p}}^{(\eta)}>\mu$, while the contribution of the inert "color"is simply $\varepsilon_{\boldsymbol{p}}^{(\eta)}-\mu$, but only for $\varepsilon_{\boldsymbol{p}}^{(\eta)}<\mu$. The gap equation in (20), i.e. $\partial\Phi(\Delta,F,\mu)/\partial\Delta=0$, is obtained as

$$\Delta\left[2\cdot\frac{1}{V}\sum_{\boldsymbol{p}\eta=\pm}^{\Lambda}\frac{1}{\sqrt{(\varepsilon_{\boldsymbol{p}}^{(\eta)}-\mu)^2+3\Delta^2}}-\frac{1}{G_c}\right]=0. \tag{26}$$

4. Numerical results and discussions

In this section, first, we investigate the possible phases with $F = 0$ and $\Delta \neq 0$ or with $F \neq 0$ and $\Delta = 0$ at high density, namely, two-flavor color superconducting phase or spin polarized phase, separately. First, as an extreme situation in the quark spin polarized phase with $\Delta = 0$, the thermodynamic potential reduces to

$$\Phi(\Delta = 0, F, \mu) = 6 \cdot \frac{1}{V} \sum_{\boldsymbol{p}\ (\varepsilon_{\boldsymbol{p}}^{(+)} \leq \mu)} (\varepsilon_{\boldsymbol{p}}^{(+)} - \mu) + 6 \cdot \frac{1}{V} \sum_{\boldsymbol{p}\ (\varepsilon_{\boldsymbol{p}}^{(-)} \leq \mu)} (\varepsilon_{\boldsymbol{p}}^{(-)} - \mu) + \frac{F^2}{2G}, \tag{27}$$

where it should be noted that $\sqrt{(\varepsilon_{\boldsymbol{p}}^{(\eta)} - \mu)^2} = \varepsilon_{\boldsymbol{p}}^{(\eta)} - \mu$ for $\varepsilon_{\boldsymbol{p}}^{(\eta)} > \mu$ or $-(\varepsilon_{\boldsymbol{p}}^{(\eta)} - \mu)$ for $\varepsilon_{\boldsymbol{p}}^{(\eta)} < \mu$, respectively, when (27) is derived from (25). Of course, the sum over momentum is replaced by the momentum-integration as

$$\frac{1}{V} \sum_{\boldsymbol{p}} \longrightarrow \int \frac{d^3\boldsymbol{p}}{(2\pi)^3}. \tag{28}$$

Then, the thermodynamic potential derived here is identical with the one that has been previously obtained by the present authors, i.e., Eq. (3.1) in Ref. [1].[2] Thus, the thermodynamic potential with $\Delta = 0$ has already been given in Ref. [12] in the analytical form as

$$\Phi(\Delta = 0, F, \mu) = \begin{cases} \dfrac{F^2}{2G} - \dfrac{1}{\pi^2}\left[\dfrac{\sqrt{\mu^2 - F^2}}{4}(3F^2\mu + 2\mu^3) + F\mu^3 \arctan\dfrac{F}{\sqrt{\mu^2 - F^2}}\right. & \\ \qquad \left. - \dfrac{F^4}{4} \ln\dfrac{\mu + \sqrt{\mu^2 - F^2}}{F}\right] & \text{for} \quad F < \mu \\ \dfrac{F^2}{2G} - \dfrac{1}{2\pi}\mu^3 F & \text{for} \quad F > \mu \end{cases}. \tag{29}$$

If the minimum of the thermodynamical potential exists in the range of $F < \mu$, the gap equation for F is derived from $\partial\Phi(\Delta = 0, F, \mu)/\partial F = 0$, which leads to

$$F = \frac{G}{\pi^2}\left[2F\mu\sqrt{\mu^2 - F^2} + \mu^3 \arctan\frac{F}{\sqrt{\mu^2 - F^2}} - F^3 \ln\frac{\mu + \sqrt{\mu^2 - F^2}}{F}\right]. \tag{30}$$

In the other case, namely, the $F = 0$ case, the two-flavor color superconducting phase may be realized with $\Delta \neq 0$. When $F = 0$, the quasiparticle energy $\varepsilon_{\boldsymbol{p}}^{(\eta)} = p$ is obtained for $\eta = \pm$. The thermodynamic potential (25) is then evaluated as

$$\begin{aligned} \Phi(\Delta, F = 0, \mu) = {} & 4 \cdot \frac{1}{V} \sum_{p<\mu} \left(2(p - \mu) - \sqrt{(p - \mu)^2 + 3\Delta^2}\right) \\ & + 4 \cdot \frac{1}{V} \sum_{p>\mu}^{\Lambda} \left((p - \mu) - \sqrt{(p - \mu)^2 + 3\Delta^2}\right) + \frac{3\Delta^2}{2G_c}. \end{aligned} \tag{31}$$

[2] In Eq. (3.1) in Ref. [12], F-integration has to be carried out.

Table 1. Parameter set.

Λ / GeV	G / GeV^{-2}	G_c / GeV^{-2}
0.631	20.0	6.6

After replacement of the sum over momentum into momentum-integration in (28), the analytical form of the thermodynamic potential is obtained with a three-momentum cutoff parameter Λ:

$$\begin{aligned}\Phi(\Delta, F=0, \mu) = {} & \frac{3\Delta^2}{2G_c} - \frac{\mu^4}{6\pi^2} + \frac{\Lambda^4}{2\pi^2} - \frac{2\mu\Lambda^3}{3\pi^2} \\ & - \frac{1}{12\pi^2}\Bigg[(2\mu^3 - 39\Delta^2\mu)\left(\sqrt{\mu^2+3\Delta^2} - \sqrt{(\mu-\Lambda)^2+3\Delta^2}\right) \\ & + (6\Lambda^3 + 9\Delta^2\Lambda - 2\Lambda^2\mu - 2\Lambda\mu^2)\sqrt{(\mu-\Lambda)^2+3\Delta^2} \\ & + 3(12\Delta^2\mu^2 - 9\Delta^4)\ln\frac{\Lambda - \mu + \sqrt{(\mu-\Lambda)^2+3\Delta^2}}{-\mu + \sqrt{\mu^2+3\Delta^2}}\Bigg]. \end{aligned} \tag{32}$$

The gap equation becomes

$$\begin{aligned}\frac{1}{\pi^2}\Bigg[& -3\mu\sqrt{\mu^2+3\Delta^2} + (3\mu+\Lambda)\sqrt{(\mu-\Lambda)^2+3\Delta^2} \\ & + (2\mu^2 - 3\Delta^2)\ln\frac{\Lambda - \mu + \sqrt{(\mu-\Lambda)^2+3\Delta^2}}{-\mu + \sqrt{\mu^2+3\Delta^2}}\Bigg] = \frac{1}{G_c}. \end{aligned} \tag{33}$$

The quark number density ρ is calculated from the thermodynamical relation as

$$\rho = -\frac{\partial\Phi(\Delta, F, \mu)}{\partial\mu}. \tag{34}$$

In our model Hamiltonian, the model parameters are G, G_c, and Λ. In the original NJL model, the coupling strength G_S appears where $G_S = 5.5$ GeV^{-2} is adopted [19], although this parameter does not appear explicitly in the model considered here. Then, following Ref. [17], the strength of the quark-pair interaction, G_c, is taken[3] as $(G_c/2)/G_S = 0.6$. Thus, we adopt $G_c = 6.6$ GeV^{-2}. As for the three-momentum cutoff Λ, a standard value [19] is adopted here, namely, $\Lambda = 0.631$ GeV. If the tail stretching beyond the Fermi momentum of occupation number should be fully taken into account in the BCS theory, a larger value of three-momentum cutoff should be adopted, such as $\Lambda = 0.8$ GeV [18]. However, it will be later seen that the tail of the occupation number is already sufficiently taken into account in the case $\Lambda = 0.631$ GeV. As for G in the strength of the tensor-type interaction between quarks, we put $G = 20$ GeV^{-2}, which was used in our previous paper [12]. As was discussed in Ref. [12], if the effect of the vacuum polarization is taken into account, the coupling constant G should be replaced with the renormalized coupling G_r, in which $1/G_r = 1/G - \Lambda^2/\pi^2$. Then, $G_r = 20$ GeV^{-2} corresponds to the bare coupling $G = 11.1$ GeV^{-2} for $\Lambda = 0.631$ GeV or $G = 8.7$ GeV^{-2} for $\Lambda = 0.8$ GeV. Thus, the strengths of the quark-pairing and tensor-type interactions are comparable. The parameter set used here is summarized in Table 1.

[3] In Ref. [17], $G_C/G_S = 0.6$ is adopted, where G_C in Ref. [17] corresponds to $G_c/2$ here.

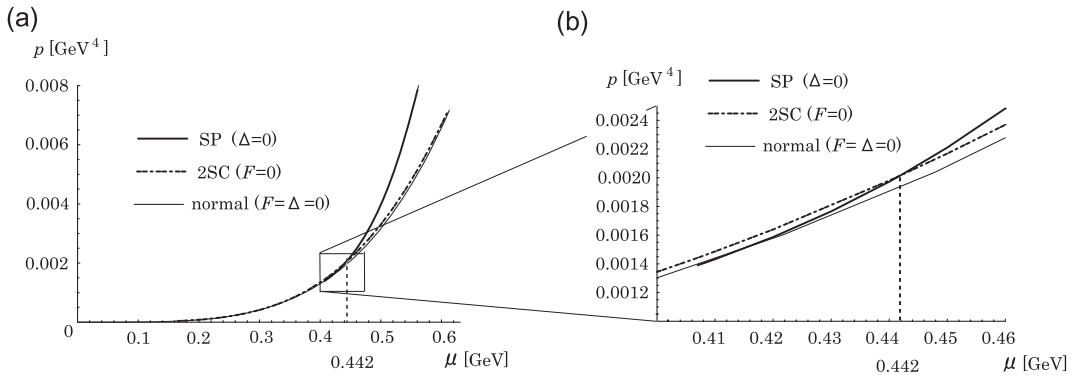

Fig. 1. (a) The pressures for normal (thin curve), two-flavor color superconducting (2SC) (dash-dotted curve), and quark spin polarized (SP) (solid curve) phases are shown as functions with respect to quark chemical potential μ in the case of $\Lambda = 0.631$ GeV. (b) The details are depicted around $\mu \approx 0.442$ GeV.

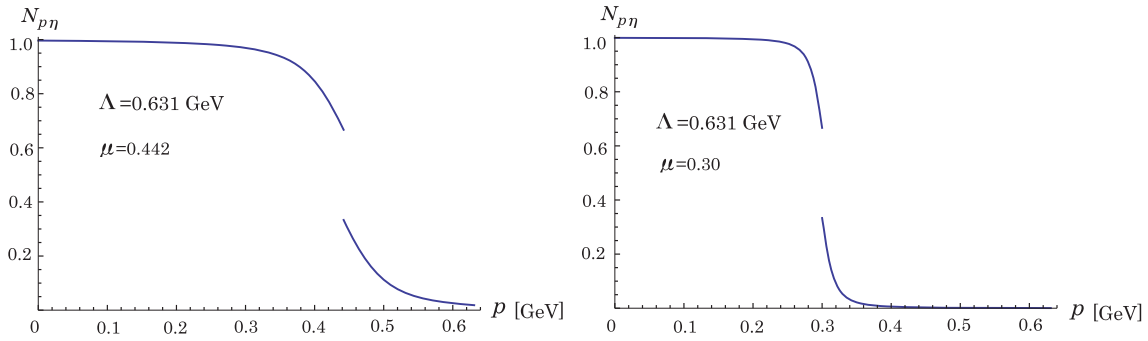

Fig. 2. The occupation number is depicted as a function of $|\boldsymbol{p}|$ in the cases $\mu = 0.442$ GeV and $\mu = 0.30$ GeV.

First, let us estimate the thermodynamic potential numerically in two phases, namely, color superconducting phase with $F = 0$ and $\Delta \neq 0$ and quark spin polarized phase with $F \neq 0$ and $\Delta = 0$, separately. The state with $(F = 0, \Delta = \Delta_0)$ gives a local minimum of the thermodynamic potential, where Δ_0 is the solution of the gap equation (26) with $F = 0$ or Eq. (33). However, the state with $(F = F_0, \Delta = 0)$ gives a local minimum or a saddle point of the thermodynamic potential corresponding to the value of μ, where F_0 is the solution of the gap equation $\partial\Phi(\Delta = 0, F, \mu)/\partial F = 0$ or Eq. (30). This is shown in Appendix C. We compare the pressure in the color superconducting phase $(F = 0, \Delta = \Delta_0)$ with that in the quark spin polarized phase $(F = F_0, \Delta = 0)$. The pressure p is given by

$$p = -\Phi(\Delta, F, \mu). \tag{35}$$

In Fig. 1(a), the pressures for normal (thin curve), two-flavor color superconducting (dash-dotted curve), and quark spin polarized (solid curve) phases are shown in the case of $\Lambda = 0.631$ GeV as functions with respect to quark chemical potential μ. Up to $\mu = \mu_c = 0.442$ GeV, where $\Phi(\Delta = \Delta_0, F = 0, \mu_c) = \Phi(\Delta = 0, F = F_0, \mu_c)$, the two-flavor color superconducting (2SC) phase is realized. However, above $\mu = \mu_c$, the quark spin polarized phase is favored. In Fig. 1(b), details are depicted around $\mu \approx 0.442(= \mu_c)$ GeV. As for the baryon number density, up to $\rho_B = 4.73\rho_0$, where $\rho_0 = 0.17$ fm^{-3} is the normal nuclear matter density, the color superconducting phase is realized. Thus, it is enough to include the effects of the tail of the occupation number with the three-momentum cutoff $\Lambda = 0.631$ GeV. In Fig. 2, the occupation number is depicted as a function of the magnitude

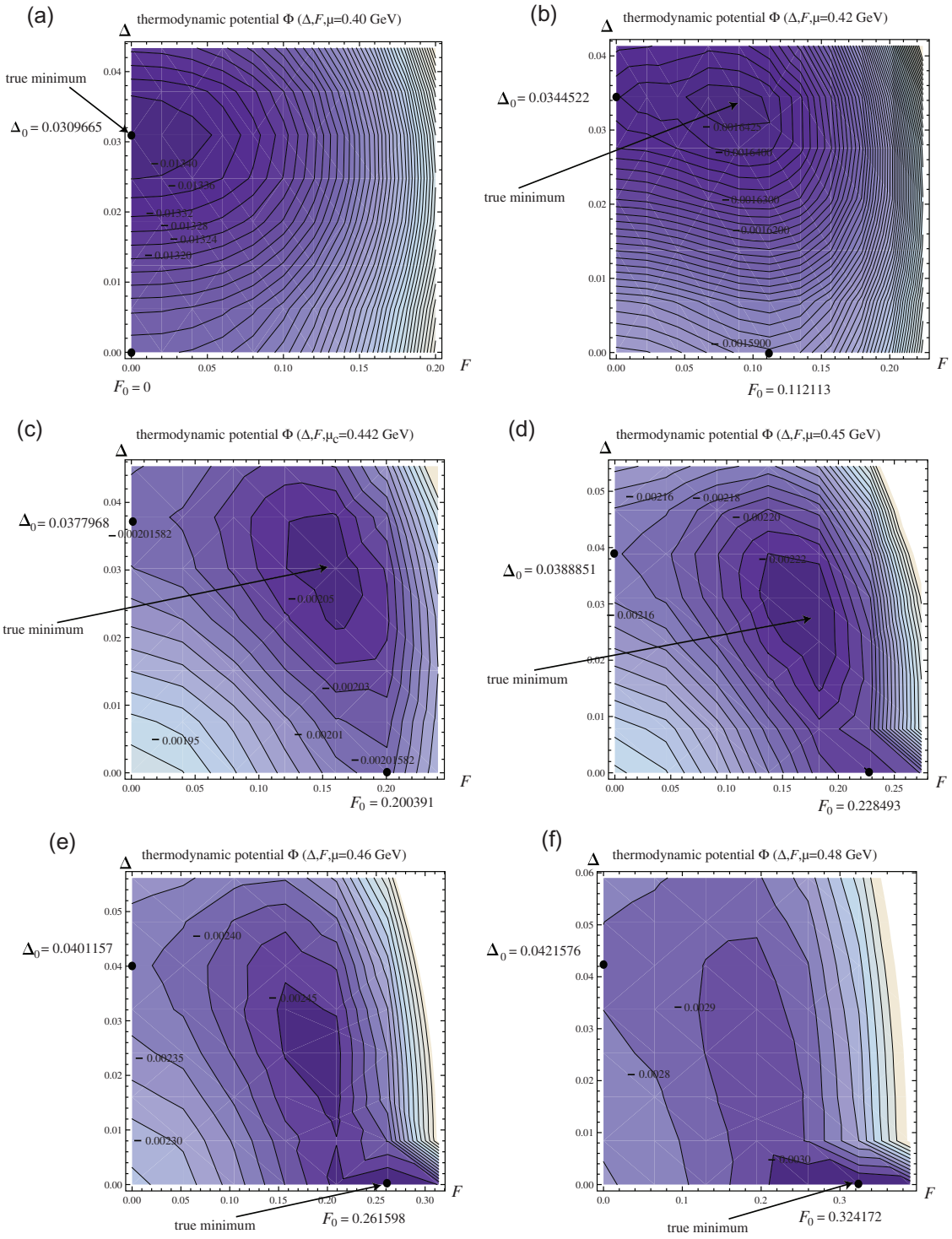

Fig. 3. The contour map of the thermodynamic potential $\Phi(\Delta, F, \mu)$ is depicted in the cases (a) $\mu = 0.40$ GeV, (b) $\mu = 0.42$ GeV, (c) $\mu = 0.442$ GeV, (d) $\mu = 0.45$ GeV, (e) $\mu = 0.46$ GeV, and (f) $\mu = 0.48$ GeV. The horizontal and vertical axes represent F and Δ, respectively.

of momentum $p(=|\boldsymbol{p}|)$. It seems from Fig. 2 that the effects of the tail of the occupation number are fully taken into account.

Secondly, let us consider the gap Δ and F simultaneously. Figure 3 shows contour maps of the thermodynamic potential $\Phi(\Delta, F, \mu)$, where the horizontal and vertical axis represent F and Δ, respectively, in the cases (a) $\mu = 0.40$ GeV, (b) $\mu = 0.42$ GeV, (c) $\mu = \mu_c = 0.442$ GeV, (d) $\mu = 0.45$ GeV, (e) $\mu = 0.46$ GeV, and (f) $\mu = 0.48$ GeV. In case (a), the gap equations give $F = 0$ and $\Delta = \Delta_0$. The point $(F = 0, \Delta = \Delta_0)$ is a true minimum of the thermodynamic potential. Then, up to $\mu \approx 0.40$ GeV, the color superconducting phase is realized. In the region with $\mu \gtrsim 0.407$ GeV, which corresponds to the baryon number density ρ divided by the normal nuclear matter density ρ_0, being $\rho/\rho_0 = 3.71$, the gap equation $\partial\Phi(\Delta = 0, F, \mu)/\partial F$ has a nontrivial solution with a nonzero F value. Then, the true minimum of the thermodynamic potential moves to the point $(F \neq 0, \Delta \approx \Delta_0)$ from the point $(F = 0, \Delta = \Delta_0)$, as is seen in Fig. 3(b). In Fig. 3(c) with $\mu = \mu_c = 0.442$ GeV, in which $\Phi(\Delta = \Delta_0, F = 0, \mu = \mu_c) = \Phi(\Delta = 0, F = F_0, \mu = \mu_c)$, the true minimum is located at $(F \approx 0.8F_0,\ \Delta \approx 0.8\Delta_0)$. This state may be interpreted as a state in a mixed phase, in the sense that this phase is intermediate between a pure spin polarized phase and a pure 2SC one. Further, in case (d), $\mu = 0.45$ GeV, the true minimum is located at $(F \approx 0.8F_0,\ \Delta \approx 0.7\Delta_0)$. In cases (e) and (f), namely $\mu \gtrsim 0.46$ GeV, the point $(F = F_0, \Delta = 0)$ becomes a true minimum and the spin polarized phase is realized. However, in case (e), two minima appear. As seen in case (e), it is most likely that a jump occurs from $(F = F_0, \Delta = \Delta_0)$ to $(F = F_0, \Delta = 0)$. Thus, starting from the 2SC phase, the second-order phase transition starts at the onset of the spin polarization $F = F_0$, and finally it seems that the transition occurs from intermediate phase to spin polarized phase.

5. Summary and concluding remarks

In this paper, it was shown within the mean field approximation that the quark spin polarized phase may be realized after the two-flavor color superconducting phase and the mixed phase as the baryon density increases. We first calculated the pressure of the two phases separately, namely, in the 2SC ($\Delta \neq 0$ and $F = 0$) and the quark spin polarized ($\Delta = 0$ and $F \neq 0$) phases. As a result, in a certain lower density region, the 2SC phase is realized. However, in rather high density regions, the quark spin polarized phase is realized. If the large F expansion is carried out in Eq. (26), then the gap equation for Δ is expressed approximately as

$$\Delta \left[\int \frac{d^3\boldsymbol{p}}{(2\pi)^3} \left(1 + \frac{2\mu\sqrt{p_1^2 + p_2^2} - 3\Delta^2}{2F^2} \right) - \frac{F}{4G_c} \right] \approx 0. \tag{36}$$

For large F, the above equation has only the trivial solution $\Delta = 0$. Thus, it is expected that in fact the quark spin polarized phase with $\Delta = 0$ and $F \neq 0$ is realized in the high baryon density region with large F. The situation is the same even if another parameter is reasonably adopted. For example, when we adopt $G = 10\ \text{GeV}^{-2}$, which is one-half of the value used in this paper, the behavior of the phase transition is similar in the case of $G = 20\ \text{GeV}^{-2}$ except for the value of chemical potential $\mu = \mu_c = 0.605$ GeV, where $\Phi(\Delta = \Delta_0, F = 0, \mu_c) = \Phi(\Delta = 0, F = F_0, \mu_c)$ is satisfied. But since $\mu_c = 0.605$ GeV is close to the three-momentum cutoff Λ, it may be impossible to draw definite conclusions about the phase transition.

It might be thought that, as a result, the spin polarized (SP) phase may be more favorable than the two-flavor color superconducting (2SC) phase at high density. It should be noted that the thermodynamic potential can be re-expressed as $\Phi = -\int_0^\mu d\mu\ N$, which is proportional to $-\mu\times$

(volume surrounded by the Fermi surface). In the quark matter with $F = 0$ at low baryon density or small quark chemical potential, the thermodynamic potential depends on μ^4 ($= \mu \times \mu^3$), namely $\Phi \propto -\mu^4$, in which μ^3 is nothing but the volume surrounded by the Fermi surface because the shape of the Fermi surface is a sphere. However, at very high baryon density or large quark chemical potential, in which the relation $F > \mu$ is satisfied, the shape of the Fermi surface becomes a torus, namely, $(\sqrt{p_1^2 + p_2^2} - F)^2 + p_3^2 = \mu^2$. Here, the volume of the torus is $2\pi^2\mu^2 \times F$, where μ is the smaller radius and F is the other larger radius of the torus. In the case $F > \mu$, namely the full polarization case, from Eq. (29), $F = (G/(2\pi)) \times \mu^3$ gives the minimum of the thermodynamic potential. As a result, the thermodynamic potential is proportional to $-\mu\times$ (volume surrounded by the Fermi surface) $\propto -\mu \times \mu^2 \times F \propto -\mu^6$, as shown in our previous paper [12]. Thus, at high baryon density or large quark chemical potential, the spin polarized phase is favored. It might be concluded that the mechanism that causes the SP phase to be more favored than the 2SC phase at high densities is the distortion effect of the Fermi surface.

For the three-momentum cutoff $\Lambda = 0.631$ GeV, it is sufficient to take into account the tail of the occupation number since the values of the chemical potential on the phase transition point from the 2SC phase to the mixed phase and from the mixed phase to the spin polarized phase are about 0.407 GeV and 0.46 GeV, respectively. In general, in the system with finite chemical potential, a chemical-potential dependent cutoff may be used [20–22]. However, for the sake of comparison, if a rather large fixed value of the three-momentum cutoff, $\Lambda = 0.8$ GeV, is adopted where the tail of the occupation number is more fully taken into account, the critical chemical potential from the 2SC phase to the mixed phase is unchanged. Above $\mu = \mu_c = 0.491$ GeV, the state with ($F = F_0$, $\Delta = 0$) is favored against the state with ($F = 0$, $\Delta = \Delta_0$). With this larger fixed three-momentum cutoff, it is concluded that, up to $\rho_B = 7.42\rho_0$, the color superconducting phase is realized. The use of a large three-momentum cutoff leads to the shift of the phase transition density, i.e., the phase transition density is higher with a larger three-momentum cutoff. However, if a larger Λ is used, it is necessary to re-adjust the coupling constants.

Secondly, the quark-pairing gap Δ and the spin polarization F were considered simultaneously. Under the present treatment, the phase transition behavior from the 2SC phase with $\Delta \neq 0$ and $F = 0$ to the quark spin polarized phase with $\Delta = 0$ and $F \neq 0$ may be clear and the transition occurs passing through the state with ($F \neq 0$, $\Delta \neq 0$), which can be interpreted as the mixed phase.

In future work, it would be interesting and important to investigate the phase equilibrium at finite temperature and in the presence of an external magnetic field. Also, matter in beta equilibrium could be analyzed, while symmetric matter is considered in the present paper. Additionally, it is important to investigate the interplay between the color-flavor locked (CFL) phase and the spin polarized phase in higher density regions in quark matter. Further, it may be interesting to investigate the interplay between two quark spin polarized phases, namely, the quark spin polarized phase originating from the tensor-type four-point interaction and that originating from the pseudovector-type four-point interaction between quarks. In this paper, the mean field approximation for the established BCS theory is adopted, under which the thermodynamic potential is considered in the standard manner. Of course, there are other approaches to investigating the phase transition, such as with the use of the CJT potential [23], the Landau potential [24], and so on. It would be interesting to clarify the difference between the standard BCS mean field approach and the CJT potential approach, including the effects of two-loop order as a general problem of the phase transition phenomena. However, that is beyond the scope of the present paper. These topics are left for future investigations.

Acknowledgements

One of the authors (Y.T.) would like to express his sincere thanks to Professor J. da Providência and Professor C. Providência, two of the co-authors of this paper, for their warm hospitality during his visit to Coimbra in summer of 2012. One of the authors (Y.T.) is partially supported by Grants-in-Aid for Scientific Research (No. 23540311) from the Ministry of Education, Culture, Sports, Science and Technology in Japan.

Appendix A. Mean field Hamiltonian in the basis of good helicity states

The following matrix is introduced in order to diagonalize the Hamiltonian matrix in Eq. (8) with Eq. (10):

$$V(\boldsymbol{p}) = \begin{pmatrix} \frac{\sqrt{\varepsilon_p^{(+)}+e+q}}{2\sqrt{\varepsilon_p^{(+)}}} & -\frac{\sqrt{\varepsilon_p^{(-)}-e+q}}{2\sqrt{\varepsilon_p^{(-)}}} & -\frac{\sqrt{\varepsilon_p^{(+)}-e-q}}{2\sqrt{\varepsilon_p^{(+)}}} & \frac{\sqrt{\varepsilon_p^{(-)}+e-q}}{2\sqrt{\varepsilon_p^{(-)}}} \\ \frac{\sqrt{\varepsilon_p^{(+)}+e+q}}{2\sqrt{\varepsilon_p^{(+)}}} & \frac{\sqrt{\varepsilon_p^{(-)}-e+q}}{2\sqrt{\varepsilon_p^{(-)}}} & -\frac{\sqrt{\varepsilon_p^{(+)}-e-q}}{2\sqrt{\varepsilon_p^{(+)}}} & -\frac{\sqrt{\varepsilon_p^{(-)}+e-q}}{2\sqrt{\varepsilon_p^{(-)}}} \\ -\frac{g}{2\sqrt{\varepsilon_p^{(+)}(\varepsilon_p^{(+)}+e+q)}} & \frac{g}{2\sqrt{\varepsilon_p^{(-)}(\varepsilon_p^{(-)}-e+q)}} & -\frac{g}{2\sqrt{\varepsilon_p^{(+)}(\varepsilon_p^{(+)}-e-q)}} & \frac{g}{2\sqrt{\varepsilon_p^{(-)}(\varepsilon_p^{(-)}+e-q)}} \\ \frac{g}{2\sqrt{\varepsilon_p^{(+)}(\varepsilon_p^{(+)}+e+q)}} & \frac{g}{2\sqrt{\varepsilon_p^{(-)}(\varepsilon_p^{(-)}-e+q)}} & \frac{g}{2\sqrt{\varepsilon_p^{(+)}(\varepsilon_p^{(+)}-e-q)}} & \frac{g}{2\sqrt{\varepsilon_p^{(-)}(\varepsilon_p^{(-)}+e-q)}} \end{pmatrix}. \quad \text{(A1)}$$

Then, we can diagonalize the Hamiltonian matrix κ as $V^\dagger \kappa V$. Namely,

$$H_{\mathrm{MF}}^{\mathrm{SP}} = \sum_{\boldsymbol{p}\tau\alpha} \begin{pmatrix} b^\dagger_{\boldsymbol{p}+\tau\alpha} \\ b^\dagger_{\boldsymbol{p}-\tau\alpha} \\ \tilde{b}^\dagger_{\boldsymbol{p}+\tau\alpha} \\ \tilde{b}^\dagger_{\boldsymbol{p}-\tau\alpha} \end{pmatrix}^T \mathrm{diag}\,\kappa \begin{pmatrix} b_{\boldsymbol{p}+\tau\alpha} \\ b_{\boldsymbol{p}-\tau\alpha} \\ \tilde{b}_{\boldsymbol{p}+\tau\alpha} \\ \tilde{b}_{\boldsymbol{p}-\tau\alpha} \end{pmatrix}, \quad \text{(A2)}$$

where we define

$$\mathrm{diag}\,\kappa = \begin{pmatrix} \varepsilon_{\boldsymbol{p}}^{(+)} & 0 & 0 & 0 \\ 0 & \varepsilon_{\boldsymbol{p}}^{(-)} & 0 & 0 \\ 0 & 0 & -\varepsilon_{\boldsymbol{p}}^{(+)} & 0 \\ 0 & 0 & 0 & -\varepsilon_{\boldsymbol{p}}^{(-)} \end{pmatrix},$$

$$\begin{pmatrix} b_{\boldsymbol{p}+\tau\alpha} \\ b_{\boldsymbol{p}-\tau\alpha} \\ \tilde{b}_{\boldsymbol{p}+\tau\alpha} \\ \tilde{b}_{\boldsymbol{p}-\tau\alpha} \end{pmatrix} = V^\dagger(\boldsymbol{p}) \begin{pmatrix} c_{\boldsymbol{p}+\tau\alpha} \\ c_{\boldsymbol{p}-\tau\alpha} \\ \tilde{c}_{\boldsymbol{p}+\tau\alpha} \\ \tilde{c}_{\boldsymbol{p}-\tau\alpha} \end{pmatrix}. \quad \text{(A3)}$$

Secondly, let us consider the total Hamiltonian matrix with the quark-pair interaction term in the basis derived above. In this basis, V_{cs} in (9) is written as

$$V_{cs} = \Delta \sum_{\boldsymbol{p}\alpha\alpha'\alpha''} \begin{pmatrix} b^\dagger_{\boldsymbol{p}++\alpha} \\ b^\dagger_{\boldsymbol{p}--\alpha} \\ \tilde{b}^\dagger_{\boldsymbol{p}++\alpha} \\ \tilde{b}^\dagger_{\boldsymbol{p}--\alpha} \end{pmatrix}^T V^\dagger(\boldsymbol{p}) V(-\boldsymbol{p}) \begin{pmatrix} b^\dagger_{-\boldsymbol{p}+-\alpha'} \\ b^\dagger_{-\boldsymbol{p}--\alpha'} \\ \tilde{b}^\dagger_{-\boldsymbol{p}+-\alpha'} \\ \tilde{b}^\dagger_{-\boldsymbol{p}--\alpha'} \end{pmatrix} \epsilon_{\alpha\alpha'\alpha''}\,. \quad \text{(A4)}$$

Here, if we replace $\boldsymbol{p}$ with $-\boldsymbol{p}$, then q, e, g, and $\varepsilon_{\boldsymbol{p}}^{(\pm)}$ in (10) are changed or unchanged to q, e, $-g$, and $\varepsilon_{\boldsymbol{p}}^{(\pm)}$. Thus, we obtain

$$V^{\dagger}(\boldsymbol{p})V(-\boldsymbol{p}) = \begin{pmatrix} \frac{q+e}{\varepsilon_{\boldsymbol{p}}^{(+)}} & 0 & -\frac{|g|}{\varepsilon_{\boldsymbol{p}}^{(+)}} & 0 \\ 0 & \frac{q-e}{\varepsilon_{\boldsymbol{p}}^{(-)}} & 0 & -\frac{|g|}{\varepsilon_{\boldsymbol{p}}^{(-)}} \\ -\frac{|g|}{\varepsilon_{\boldsymbol{p}}^{(+)}} & 0 & -\frac{q+e}{\varepsilon_{\boldsymbol{p}}^{(+)}} & 0 \\ 0 & -\frac{|g|}{\varepsilon_{\boldsymbol{p}}^{(-)}} & 0 & -\frac{q-e}{\varepsilon_{\boldsymbol{p}}^{(-)}} \end{pmatrix}. \tag{A5}$$

Finally, let us diagonalize the above matrix $V^{\dagger}(\boldsymbol{p})V(-\boldsymbol{p})$. We introduce the following matrix:

$$W = \begin{pmatrix} -\sqrt{\frac{\varepsilon_{\boldsymbol{p}}^{(+)}+e+q}{2\varepsilon_{\boldsymbol{p}}^{(+)}}} & 0 & \sqrt{\frac{\varepsilon_{\boldsymbol{p}}^{(+)}-e-q}{2\varepsilon_{\boldsymbol{p}}^{(+)}}} & 0 \\ 0 & -\sqrt{\frac{\varepsilon_{\boldsymbol{p}}^{(-)}-e+q}{2\varepsilon_{\boldsymbol{p}}^{(-)}}} & 0 & \sqrt{\frac{\varepsilon_{\boldsymbol{p}}^{(-)}+e-q}{2\varepsilon_{\boldsymbol{p}}^{(-)}}} \\ \frac{|g|}{\sqrt{2\varepsilon_{\boldsymbol{p}}^{(+)}(\varepsilon_{\boldsymbol{p}}^{(+)}+e+q)}} & 0 & \frac{|g|}{\sqrt{2\varepsilon_{\boldsymbol{p}}^{(+)}(\varepsilon_{\boldsymbol{p}}^{(+)}-e-q)}} & 0 \\ 0 & \frac{|g|}{\sqrt{2\varepsilon_{\boldsymbol{p}}^{(-)}(\varepsilon_{\boldsymbol{p}}^{(-)}-e+q)}} & 0 & \frac{|g|}{\sqrt{2\varepsilon_{\boldsymbol{p}}^{(-)}(\varepsilon_{\boldsymbol{p}}^{(-)}+e-q)}} \end{pmatrix}. \tag{A6}$$

Then, by using the matrix W, the matrix $V^{\dagger}(\boldsymbol{p})V(-\boldsymbol{p})$ that appears in the quark-pair interaction part can be diagonalized as

$$W^{\dagger}V^{\dagger}(\boldsymbol{p})V(-\boldsymbol{p})W = \begin{pmatrix} 1 & 0 & 0 & 0 \\ 0 & 1 & 0 & 0 \\ 0 & 0 & -1 & 0 \\ 0 & 0 & 0 & -1 \end{pmatrix}. \tag{A7}$$

By introducing new fermion operators ($a_{\boldsymbol{p}\eta\tau\alpha}$, $a^{\dagger}_{\boldsymbol{p}\eta\tau\alpha}$, $\tilde{a}_{\boldsymbol{p}\eta\tau\alpha}$, $\tilde{a}^{\dagger}_{\boldsymbol{p}\eta\tau\alpha}$) by

$$\begin{pmatrix} a_{\boldsymbol{p}+\tau\alpha} \\ a_{\boldsymbol{p}-\tau\alpha} \\ \tilde{a}_{\boldsymbol{p}+\tau\alpha} \\ \tilde{a}_{\boldsymbol{p}-\tau\alpha} \end{pmatrix} = W^{\dagger} \begin{pmatrix} b_{\boldsymbol{p}+\tau\alpha} \\ b_{\boldsymbol{p}-\tau\alpha} \\ \tilde{b}_{\boldsymbol{p}+\tau\alpha} \\ \tilde{b}_{\boldsymbol{p}-\tau\alpha} \end{pmatrix}, \tag{A8}$$

the mean field Hamiltonian in which both quark spin polarization and the quark-pair condensate are simultaneously considered can be expressed in Eq. (13).

Appendix B. Expectation values of bilinear operators with respect to the BCS state

The expectation values for the BCS state are summarized as follows:

$$\begin{aligned} X_{\boldsymbol{p}\eta} &= \langle\Psi|a^{\dagger}_{\boldsymbol{p}\eta\tau\alpha}a_{\boldsymbol{p}\eta\tau\alpha'}|\Psi\rangle\,, \qquad (\text{for} \quad \alpha \neq \alpha') \\ N_{\boldsymbol{p}\eta} &= \langle\Psi|a^{\dagger}_{\boldsymbol{p}\eta\tau\alpha}a_{\boldsymbol{p}\eta\tau\alpha}|\Psi\rangle\,, \\ D_{\boldsymbol{p}\eta} &= \langle\Psi|a_{-\boldsymbol{p}\eta-\tau\alpha'}a_{\boldsymbol{p}\eta\tau\alpha}|\Psi\rangle\,, \qquad (\text{for} \quad \alpha \neq \alpha') \\ P_{\boldsymbol{p}\eta} &= \langle\Psi|a_{-\boldsymbol{p}\eta-\tau\alpha}a_{\boldsymbol{p}\eta\tau\alpha}|\Psi\rangle, \end{aligned} \tag{B1}$$

where we take $\alpha = 1$ and $\alpha' = 2$ for the following calculations because color symmetry is retained. We can easily calculate the above expectation values by using the relation (16) with (15).

For $\varepsilon_{\boldsymbol{p}}^{(\eta)} > \mu$, the following relations are obtained:

$$\begin{aligned} X_{\boldsymbol{p}\eta} &= -K_{\boldsymbol{p}\eta}^2 + K_{\boldsymbol{p}\eta}^2 (N_{\boldsymbol{p}\eta} - X_{\boldsymbol{p}\eta}), \\ N_{\boldsymbol{p}\eta} &= 2K_{\boldsymbol{p}\eta}^2 - 2K_{\boldsymbol{p}\eta}^2 (N_{\boldsymbol{p}\eta} - X_{\boldsymbol{p}\eta}), \\ D_{\boldsymbol{p}\eta} &= K_{\boldsymbol{p}\eta} - 3K_{\boldsymbol{p}\eta}^2 D_{\boldsymbol{p}\eta} + K_{\boldsymbol{p}\eta}^2 P_{\boldsymbol{p}\eta}, \\ P_{\boldsymbol{p}\eta} &= -2K_{\boldsymbol{p}\eta}^2 P_{\boldsymbol{p}\eta}. \end{aligned} \tag{B2}$$

In the same way, for $\varepsilon_{\boldsymbol{p}}^{(\eta)} \leq \mu$, the following relations are also obtained:

$$\begin{aligned} X_{\boldsymbol{p}\eta} &= -\widetilde{K}_{\boldsymbol{p}\eta}^2 (X_{\boldsymbol{p}\eta} - N_{\boldsymbol{p}\eta}), \\ N_{\boldsymbol{p}\eta} &= 1 + 2\widetilde{K}_{\boldsymbol{p}\eta}^2 (X_{\boldsymbol{p}\eta} - N_{\boldsymbol{p}\eta}), \\ D_{\boldsymbol{p}\eta} &= \widetilde{K}_{\boldsymbol{p}\eta} - 3\widetilde{K}_{\boldsymbol{p}\eta}^2 D_{\boldsymbol{p}\eta} - \widetilde{K}_{\boldsymbol{p}\eta}^2 P_{\boldsymbol{p}\eta}, \\ P_{\boldsymbol{p}\eta} &= 2\widetilde{K}_{\boldsymbol{p}\eta}^2 P_{\boldsymbol{p}\eta}. \end{aligned} \tag{B3}$$

As a result, the expectation values are calculated as

For $\varepsilon_{\boldsymbol{p}}^{(\eta)} > \mu$

$$X_{\boldsymbol{p}\eta} = -\frac{K_{\boldsymbol{p}\eta}^2}{1 + 3K_{\boldsymbol{p}\eta}^2}, \quad N_{\boldsymbol{p}\eta} = \frac{2K_{\boldsymbol{p}\eta}^2}{1 + 3K_{\boldsymbol{p}\eta}^2}, \quad D_{\boldsymbol{p}\eta} = \frac{K_{\boldsymbol{p}\eta}}{1 + 3K_{\boldsymbol{p}\eta}^2}, \quad P_{\boldsymbol{p}\eta} = 0, \tag{B4}$$

For $\varepsilon_{\boldsymbol{p}}^{(\eta)} \leq \mu$

$$\begin{aligned} X_{\boldsymbol{p}\eta} &= \frac{\widetilde{K}_{\boldsymbol{p}\eta}^2}{1 + 3\widetilde{K}_{\boldsymbol{p}\eta}^2}, \quad N_{\boldsymbol{p}\eta} = \frac{1 + \widetilde{K}_{\boldsymbol{p}\eta}^2}{1 + 3K_{\boldsymbol{p}\eta}^2} = 1 - \frac{2\widetilde{K}_{\boldsymbol{p}\eta}^2}{1 + 3\widetilde{K}_{\boldsymbol{p}\eta}^2}, \\ D_{\boldsymbol{p}\eta} &= \frac{\widetilde{K}_{\boldsymbol{p}\eta}}{1 + 3\widetilde{K}_{\boldsymbol{p}\eta}^2}, \quad P_{\boldsymbol{p}\eta} = 0. \end{aligned} \tag{B5}$$

Appendix C. The states with ($\Delta \neq 0$, $F = 0$) and ($\Delta = 0$, $F \neq 0$)

It may be shown that $(\Delta_0, F = 0)$ is a local minimum of the thermodynamic potential $\Phi(\Delta, F, \mu)$, where Δ_0 is the solution of the gap equation $\partial\Phi(\Delta, F = 0)/\partial\Delta = 0$. Here, the states with $(\Delta_0, F = 0)$ and $(\Delta = 0, F_0)$ give extrema of the thermodynamic potential, where F_0 is the solution of the gap equation $\partial\Phi(\Delta = 0, F)/\partial F = 0$:

$$\frac{\partial\Phi(\Delta, F, \mu)}{\partial\Delta} = 3\Delta \left[-2 \cdot \frac{1}{V} \sum_{\boldsymbol{p},\eta}^{\Lambda} \frac{1}{\sqrt{(\varepsilon_{\boldsymbol{p}}^{(\eta)} - \mu)^2 + 3\Delta^2}} + \frac{1}{G_c} \right], \tag{C1}$$

$$\begin{cases} \dfrac{\partial\Phi(\Delta_0, F=0, \mu)}{\partial\Delta} = 0, & \text{(gap equation)} \\ \dfrac{\partial\Phi(\Delta=0, F, \mu)}{\partial\Delta} = 0, \end{cases}$$

$$\begin{aligned} \frac{\partial\Phi(\Delta, F, \mu)}{\partial F} &= 2\cdot\frac{1}{V}\sum_{\boldsymbol{p},\eta,\varepsilon_{\boldsymbol{p}}\le\mu}\left[2-\frac{\varepsilon_{\boldsymbol{p}}^{(\eta)}-\mu}{\sqrt{(\varepsilon_{\boldsymbol{p}}^{(\eta)}-\mu)^2+3\Delta^2}}\right]\frac{\partial\varepsilon_{\boldsymbol{p}}^{(\eta)}}{\partial F} \\ &\quad + 2\cdot\frac{1}{V}\sum_{\boldsymbol{p},\eta,\varepsilon_{\boldsymbol{p}}\ge\mu}\left[1-\frac{\varepsilon_{\boldsymbol{p}}^{(\eta)}-\mu}{\sqrt{(\varepsilon_{\boldsymbol{p}}^{(\eta)}-\mu)^2+3\Delta^2}}\right]\frac{\partial\varepsilon_{\boldsymbol{p}}^{(\eta)}}{\partial F}+\frac{F}{G}, \end{aligned} \tag{C2}$$

$$\begin{cases} \dfrac{\partial\Phi(\Delta=0, F, \mu)}{\partial F} = 0, & \text{(gap equation)} \\ \dfrac{\partial\Phi(\Delta, F=0, \mu)}{\partial F} = 0, \end{cases}$$

where the last equality is satisfied due to $\partial\varepsilon_{\boldsymbol{p}}^{(\eta)}/\partial F|_{F=0} = \eta\sqrt{p_1^2+p_2^2}/p$, $\varepsilon_{\boldsymbol{p}}^{(\eta)} = |\boldsymbol{p}|$, and $\eta = \pm 1$. The condition that the states corresponding to $(\Delta_0, F=0)$ or $(\Delta=0, F_0)$ are a local minima is that the eigenvalues are positive for the following stability matrix $\mathcal{M}(\Delta, F)$, which consists of the second derivatives:

$$\mathcal{M}(\Delta, F) = \begin{pmatrix} \dfrac{\partial^2\Phi(\Delta, F, \mu)}{\partial\Delta^2} & \dfrac{\partial^2\Phi(\Delta, F, \mu)}{\partial F\partial\Delta} \\ \dfrac{\partial^2\Phi(\Delta, F, \mu)}{\partial\Delta\partial F} & \dfrac{\partial^2\Phi(\Delta, F, \mu)}{\partial F^2} \end{pmatrix}, \tag{C3}$$

where

$$\frac{\partial^2\Phi(\Delta, F, \mu)}{\partial\Delta^2} = 3\left[-2\cdot\frac{1}{V}\sum_{\boldsymbol{p},\eta}^{\Lambda}\frac{(\varepsilon_{\boldsymbol{p}}^{(\eta)}-\mu)^2}{[(\varepsilon_{\boldsymbol{p}}^{(\eta)}-\mu)^2+3\Delta^2]^{3/2}}+\frac{1}{G_c}\right], \tag{C4a}$$

$$\begin{aligned} \frac{\partial^2\Phi(\Delta, F, \mu)}{\partial F^2} &= 2\cdot\frac{1}{V}\sum_{\boldsymbol{p},\eta,\varepsilon_{\boldsymbol{p}}\le\mu}\left[-\frac{3\Delta^2}{[(\varepsilon_{\boldsymbol{p}}^{(\eta)}-\mu)^2+3\Delta^2]^{3/2}}\right]\frac{\left(F+\eta\sqrt{p_1^2+p_2^2}\right)^2}{\varepsilon_{\boldsymbol{p}}^{(\eta)2}} \\ &\quad + 2\cdot\frac{1}{V}\sum_{\boldsymbol{p},\eta,\varepsilon_{\boldsymbol{p}}\le\mu}\left[2-\frac{\varepsilon_{\boldsymbol{p}}^{(\eta)}-\mu}{\sqrt{(\varepsilon_{\boldsymbol{p}}^{(\eta)}-\mu)^2+3\Delta^2}}\right]\frac{p_3^2}{\varepsilon_{\boldsymbol{p}}^{(\eta)3}} \\ &\quad + 2\cdot\frac{1}{V}\sum_{\boldsymbol{p},\eta,\varepsilon_{\boldsymbol{p}}\ge\mu}\left[-\frac{3\Delta^2}{[(\varepsilon_{\boldsymbol{p}}^{(\eta)}-\mu)^2+3\Delta^2]^{3/2}}\right]\frac{(F+\eta\sqrt{p_1^2+p_2^2})^2}{\varepsilon_{\boldsymbol{p}}^{(\eta)2}} \\ &\quad + 2\cdot\frac{1}{V}\sum_{\boldsymbol{p},\eta,\varepsilon_{\boldsymbol{p}}\ge\mu}\left[1-\frac{\varepsilon_{\boldsymbol{p}}^{(\eta)}-\mu}{\sqrt{(\varepsilon_{\boldsymbol{p}}^{(\eta)}-\mu)^2+3\Delta^2}}\right]\frac{p_3^2}{\varepsilon_{\boldsymbol{p}}^{(\eta)3}}+\frac{1}{G}, \end{aligned} \tag{C4b}$$

$$\frac{\partial^2\Phi(\Delta, F, \mu)}{\partial F\partial\Delta} = 6\Delta\cdot\frac{1}{V}\sum_{\boldsymbol{p},\eta}^{\Lambda}\frac{\varepsilon_{\boldsymbol{p}}^{(\eta)}-\mu}{[(\varepsilon_{\boldsymbol{p}}^{(\eta)}-\mu)^2+3\Delta^2]^{3/2}}\cdot\frac{F+\eta\sqrt{p_1^2+p_2^2}}{\varepsilon_{\boldsymbol{p}}^{(\eta)}}. \tag{C4c}$$

Then, if $(\Delta=\Delta_0, F=0)$ is a local minimum, the eigenvalues of the stability matrix $\mathcal{M}(\Delta_0, F=0)$ have to be positive. Here, it should be noted that $\mathcal{M}(\Delta_0, 0)$ is a diagonal matrix because

Table 2. Numerical estimations.

μ / GeV	Δ_0 / GeV	$\frac{\partial^2\Phi(\Delta_0, F=0, \mu)}{\partial F^2}$ / GeV^2
0.44	0.037 5255	0.007 743 56
0.441 90	0.037 7933	0.007 492 14
μ_c		
0.441 95	0.037 8003	0.007 485 53
0.45	0.038 8851	0.006 447 47

$\partial^2\Phi(\Delta_0, F=0, \mu)/\partial F\partial\Delta = 0$ due to $\varepsilon_{\boldsymbol{p}}^{(\eta)} = |\boldsymbol{p}|$ and $\eta = \pm 1$. Further, by using the gap equation for $\Delta(\neq 0)$, we obtain

$$\frac{\partial^2\Phi(\Delta_0, F=0, \mu)}{\partial\Delta^2} = 6\cdot\frac{1}{V}\sum_{\boldsymbol{p},\eta}^{\Lambda}\frac{3\Delta_0^2}{[(p-\mu)^2+3\Delta_0^2]^{3/2}} > 0\,. \tag{C5}$$

As for the other diagonal matrix element, $\partial^2\Phi(\Delta_0, F=0, \mu)/\partial F^2$, the positiveness is not shown analytically. Instead of analytical calculation, numerical estimation is useful just before and after the chemical potential $\mu = \mu_c$ with model parameters $G = 20$ GeV^{-2}, $G_c = 6.6$ GeV^{-2}, and $\Lambda = 0.631$ GeV used in our paper, where μ_c gives $\Phi(\Delta_0, F=0, \mu_c) = \Phi(\Delta=0, F_0, \mu_c)$. From Table 2, it is seen that the eigenvalues of the stability matrix $\mathcal{M}(\Delta_0, F=0)$ are positive together with (C5). Thus, the state with $(\Delta = \Delta_0, F=0)$ is identified with a local minimum state of the thermodynamic potential.

Next, let us consider the state with $(\Delta = 0, F_0)$. The stability matrix $\mathcal{M}(\Delta=0, F_0)$ is also a diagonal matrix. We easily obtain the inequality

$$\frac{\partial^2\Phi(\Delta=0, F_0, \mu)}{\partial F^2} = 6\cdot\frac{1}{V}\sum_{\boldsymbol{p},\eta,\varepsilon_{\boldsymbol{p}}^{(\eta)}\le\mu}\frac{p_3^2}{\varepsilon_{\boldsymbol{p}}^{(\eta)3}} + \frac{1}{G} > 0. \tag{C6}$$

As for the other matrix element, $\partial^2\Phi(\Delta=0, F_0, \mu)/\partial\Delta^2$, numerical estimation, just before and after the point $\mu = \mu_c$, may also be useful. However, the integral diverges at $\varepsilon_{\boldsymbol{p}}^{(\eta)} = \mu$. This is not surprising, in view of a well known "anomaly" of the BCS theory, according to which a perturbation expansion in powers of the coupling constant G is not valid, even if this parameter is infinitesimally small. As a result, the thermodynamical potential cannot be expanded in powers of Δ, even if this parameter is infinitesimally small. We find that $\partial\Phi(\Delta=0, F_0, \mu)/\partial\Delta = 0$, but the second derivative diverges. We wish to see if, in the Δ direction, the extremum point $(\Delta = 0, F_0)$ is a maximum or a minimum. Figure 3 shows that the point with $(\Delta = 0, F_0)$ is a minimum point in the F direction, but is a maximum point in the Δ direction in the region $\mu < 0.46$ GeV. Thus, in this region, a point $(\Delta = 0, F_0)$ is a saddle point. However, the case $\mu \gtrsim 0.46$ GeV, the extremum point with $(\Delta = 0, F_0)$ is a minimum point in the Δ direction. Thus, it is concluded that the point $(\Delta = 0, F_0)$ gives a true minimum of the thermodynamic potential Φ, which results in the quark spin polarized phase.

References

[1] K. Fukushima and T. Hatsuda, Rep. Prog. Phys. **74**, 014001 (2011).
[2] T. Kunihiro, T. Muto, T. Takatsuka, R. Tamagaki, and T. Tatsumi, Prog. Theor. Phys. Suppl. **112**, 1 (1993).
[3] M. Alford, K. Rajagopal, and F. Wilczek, Nucl. Phys. B **357**, 443 (1999).
[4] K. Iida and G. Baym, Phys. Rev. D **63**, 074018 (2001).

[5] M. G. Alford, A. Schmitt, K. Rajagopal, and T. Schafer, Rev. Mod. Phys. **80**, 1455 (2008), and references therein.
[6] L. McLerran and R. D. Pisarski, Nucl. Phys. A **796**, 83 (2007).
[7] T. Tatsumi, Phys. Lett. B **489**, 280 (2000).
[8] T. Maruyama and T. Tatsumi, Nucl. Phys. A **693**, 710 (2001).
[9] E. Nakano, T. Maruyama, and T. Tatsumi, Phys. Rev. D **68**, 105001 (2003).
[10] C. Kouveliotou et al., Nature **393**, 235 (1998).
[11] S. Maedan, Prog. Theor. Phys. **118**, 729 (2007).
[12] Y. Tsue, J. da Providência, C. Providência, and M. Yamamura, Prog. Theor. Phys. **128**, 507 (2012).
[13] H. Bohr, P. K. Panda, C. Providência, and J. da Providência, Int. J. Mod. Phys. E **22**, 1350019 (2013).
[14] H. Bohr, C. Providência, and J. da Providência, Eur. Phys. J. A **41**, 355 (2009).
[15] Y. Nambu and G. Jona-Lasinio, Phys. Rev. **122**, 345 (1961).
[16] Y. Nambu and G. Jona-Lasinio, Phys. Rev **124**, 246 (1961).
[17] M. Kitazawa, T. Koide, T. Kunihiro, and Y. Nemoto, Prog. Theor. Phys. **108**, 929 (2002).
[18] H. Bohr, P. K. Panda, C. Providência, and J. da Providência, Braz. J. Phys. **42**, 68 (2012).
[19] T. Hatsuda and T. Kunihiro, Phys. Rep. **247**, 221 (1994).
[20] C. H. Lenzi, A. S. Schneider, C. Providência, and R. M. Marinho Jr., Phys. Rev. C **82**, 015809 (2010).
[21] R. Casalbuoni, R. Gatto, G. Nardulli, and M. Ruggoeri, Phys. Rev. D **68**, 034024 (2003).
[22] M. Baldo, G. F. Burgio, P. Castorina, S. Plumari, and Z. Zappalà, Phys. Rev. C **75**, 035804 (2007).
[23] J. M. Cornwall, R. Jackiw, and E. Tombolis, Phys. Rev. D **10**, 2428 (1974).
[24] Y. Hashimoto, Y. Tsue, and H. Fujii, Prog. Theor. Phys. **114**, 595 (2005).